Journal of the Serbian Chemical Society
JSCS-info@shd.org.rs • www.shd.org.rs/JSCS

ACCEPTED MANUSCRIPT

This is an early electronic version of an as-received manuscript that has been accepted for publication in the Journal of the Serbian Chemical Society but has not yet been subjected to the editing process and publishing procedure applied by the JSCS Editorial Office.

Please cite this article as S. A. Noonari, A. S. Jamali, Q. B. Jamali, A. Q. Laghari, I. Ali, H. Shaikh, S. Ahmed, M. S. Shaikh, A. Iqbal, and M. Abro, *J. Serb. Chem. Soc.* (2026) https://doi.org/10.2298/JSC260829066N

This "raw" version of the manuscript is being provided to the authors and readers for their technical service. It must be stressed that the manuscript still has to be subjected to copyediting, typesetting, English grammar and syntax corrections, professional editing and authors' review of the galley proof before it is published in its final form. Please note that during these publishing processes, many errors may emerge which could affect the final content of the manuscript and all legal disclaimers applied according to the policies of the Journal.

Journal of the Serbian Chemical Society
JSCS-info@shd.org.rs • www.shd.org.rs/JSCS
J. Serb. Chem. Soc. **00(0)** 1-16 (2026)
JSCS–14166
Original scientific paper
Published DD MM, 2026

Accepted manuscript

Post-weld heat treatment effects on shielded metal arc welded dissimilar AISI 201/4140 welds

SHOUKAT ALI NOONARI[1]*, ABDUL SATTAR JAMALI[1], QADIR BAKHSH JAMALI[1], ABDUL QADEER LAGHARI[2†], IMDAD ALI[1], HAMZA SHAIKH[3], SAGHEER AHMED[4], MUHAMMAD SHUAIB SHAIKH[2], ARSHAD IQBAL[5], MASROOR ABRO[2]

[1]Mechanical Engineering Department, Quaid-e-Awam University of Engineering and Technology, Nawabshah, Pakistan, [2]Chemical Engineering Department, Mehran University of Engineering and Technology, Jamshoro, Sindh, Pakistan, [3]Mechanical Engineering Department, Mehran University of Engineering and Technology, Jamshoro, Sindh, Pakistan, [4]Mechanical Engineering Department, Isra University Hyderabad, Sindh, Pakistan, and [5]Chemical Engineering Department, Dawood University of Engineering and Technology, Karachi, Sindh, Pakistan.

(Received 29 August; revised 10 September; accepted 28 October 2026)

Abstract: Dissimilar welding of austenitic stainless steel and low alloy steel is widely employed in pressure vessels, petrochemical plants, power generation systems, and structural applications because it combines the corrosion resistance of stainless steel with the high strength of low alloy steel. However, acquiring high quality weld joints remains challenging due to differences in thermal expansion, chemical composition, and microstructural evolution. This paper examines the joint influence of electrode selection and post-weld heat treatment (PWHT) on the microstructure and mechanical properties of shielded metal arc welded (SMAW) dissimilar joint between AISI 4140 low alloy steel and AISI 201 austenitic stainless steel. Welded sample specimens were joined using E6013 and E308 electrodes and the samples were later subjected to PWHT at 600 °C, 615 °C, and 630 °C for 1 h, followed by furnace cooling. Microstructural analysis was conducted using scanning electron microscopy (SEM), while tensile and Rockwell hardness tests were conducted to evaluate the mechanical performance of the welded joints. SEM characterization showed that the welded joint using E6013 electrode formed ferritic martensitic structures in the fusion zone, whereas the E308 electrode formed an austenitic dendritic microstructure containing retained δ-ferrite. It is noted that after the PWHT of welded samples the hardness variation was reduced and the tensile properties were improved. Among the examined specimens, the specimen welded with E308 electrode with PWHT at 615 °C revealed the optimal mechanical performance, achieving an

* Corresponding authors. E-mails: shoukat.noonari88@yahoo.com; †abdul.qadeer@admin.muet.edu.pk
https://doi.org/10.2298/JSC260829066N

ultimate tensile strength of 523 MPa, a yield strength of 392 MPa, and an elongation of 44%. These improvements resulted from an effective residual stress relief and microstructural stabilization during PWHT. The findings reveal that the joint use of the E308 electrode and PWHT at 615 °C offers the most favorable balance of mechanical and microstructural stability for SMAW dissimilar welding of AISI 4140 and AISI 201 steels.

Keywords: dissimilar welding; electrode; microstructure; post-weld heat treatment; mechanical properties.

INTRODUCTION

Dissimilar metal welding (DMW) has acquired great importance in modern engineering applications because it facilitates the joining of materials with different thermal, mechanical, and corrosion-resistant properties, thereby combining the advantages of each material in a single component.[1,2] These types of joints are mostly used in petrochemical industries, power plants, automotive structures pressure vessels and aerospace components, where different sections of a component are subjected to diverse service conditions.[3] Among different dissimilar material combinations, the joining of austenitic stainless steel and low-alloy steel has attracted significant attention because it brings together the excellent corrosion resistance of stainless steel with the high strength and relatively low cost of low-alloy steel.[4,5] However, welding these dissimilar materials provides many metallurgical challenges, including carbon migration, residual stress creation, elemental dilution, martensite formation in the heat-affected zone and differences in thermal expansion coefficients, all of which may adversely impact the mechanical performance and service life of the welded joint.[6] Therefore, selecting an appropriate electrode is essential for controlling weld metal chemistry, phase evolution, and crack susceptibility, thereby improving the overall performance of dissimilar welded joints.[7] In addition, post-weld heat treatment (PWHT) is widely employed to relieve residual stresses and modify the microstructure, thereby improving the mechanical performance of welded joints.[8,9] Several studies have reported the beneficial effects of PWHT in reducing brittleness and enhancing toughness in dissimilar welds. Although dissimilar welding between stainless steels and low-alloy steels has been extensively investigated using welding processes such as GTAW, friction welding, and laser welding, previous studies have primarily focused on the influence of either electrode selection or post-weld heat treatment PWHT independently.[1°] Although several studies have investigated GTAW, friction welding and laser welding of stainless steel–low alloy steel combinations, systematic investigations on SMAW joining of AISI 201 to AISI 4140 using conventional E6013 and stainless steel E308 electrodes under multiple PWHT temperatures remain scarce. The combined analysis of electrode selection and PWHT is experimentally important because the electrode manages the phase formation and weld metal chemistry, whereas PWHT changes phase stability,

Accepted manuscript

residual stresses and microstructural evolution. Therefore, the current study determines the combined effect of E6013 and E308 electrodes jointly with PWHT at 600 °C, 615 °C, and 630 °C on the microstructure and mechanical properties of SMAW dissimilar weld joints between AISI 201 stainless steel and AISI 4140 low-alloy steel. The main novelty of this work is providing a systematic comparison of two industrially important electrodes under multiple PWHT conditions to identify the optimum electrode PWHT combination for achieving improved microstructural stability and superior mechanical performance.

MATERIALS AND METHODS

Joining dissimilar steels has become increasingly important because it enables engineers to combine the superior corrosion resistance of stainless steel with the high strength of low-alloy steel while reducing manufacturing costs. The type of stainless steel used in this research is AISI 201. This stainless steel is widely used in various industrial applications and it is good especially where corrosion resistance and moderate strength are required at lower cost as compared to AISI 304.The type of low alloy steel used is AISI 4140. This has good strength properties, its welding requires careful control because of hardenability and martensite formation. The chemical composition in terms of weight percentage for both AISI 201 and AISI 4140 have been shown in Table. I.

TABLE I. chemical composition of metals (based on weight %)

Constituents	AISI 201	AISI 4140
C	0.15	0.42
Mn	5.5-7.5	0.83
P	0.05	0.011
S	0.03	0.010
Si	0.75	0.24
Cr	16-18	0.98
Ni	3.5-5.5	0.12
Mo	-	0.16
Fe	balance	balance

Both ASS and LAS plates had dimensions of 300 mm ×150mm×6mm.A single V-groove butt joint having a 60° included groove angle and 2 mm root gap was prepared for welding of the dissimilar plates given in Figure 1.

METHODOLOGY

Proper welding techniques are required to produce defect free and mechanically sound dissimilar joints between AISI 201 stainless steel and AISI 4140 low alloy steel. There are various types of welding techniques available in industry. In this research shielded metal arc welding (SMAW) was adopted for welding these two dissimilar metals. In this study manual metal arc welding machine MMA 200T was used. Electrode selection was considered the primary experimental variable in this investigation. Various electrodes have been investigated by previous researchers for their study. One study reported that for joining mild steel and Stainless steel by using SMAW method E6012 electrode could be an option.[11] some researchers used E308L Stainless steel electrode as third metal both in Gas metal arc welding (GMAW) and

Accepted manuscript

Shielded metal arc welding (SMAW) technique.[12,13] In the present study two electrodes E6013 and E308 have been used in the Shielded metal arc welding (SMAW) technique. The chemical compositions of both electrodes are given in Table II. Due to welding, weld metal and heat-affected zone (HAZ) experience changes in microstructure and also develop residual stresses.[14,9,] To enhance the property of heat-affected zone tempering was employed as post-weld heat treatment (PWHT). In some experimental investigations, PWHT has been done at 600 °C for 2 hours which significantly improved the mechanical properties results[19] also in some other experiments different PWHT temperatures have been used to determine the effect of PWHT on the mechanical property of metal.[2o] In the High strength low alloy steel structure PWHT has been carried out at 600 °C for 1 h.[21] It is also reported in literature that cooling process is done by furnace cooling.[14–18]. In this research paper there are three different temperatures 600 °C, 615 °C and 630 °C was followed for PWHT. The holding time followed for PWHT was 1 h. The selected PWHT temperatures 600 °C, 615 °C and 630 °C were chosen based on previous investigations which reported significant stress relief and tempering effects near 600 °C for low alloy steel weldments. The choice of E6013 and E308 electrodes was based on their industrial significance and different alloy compositions. E6013 comprises a traditional low cost mild steel electrode widely used in manufacturing industries, whereas E308 is a stainless steel electrode consisting of greater nickel and chromium contents that support austenite stabilization and increase crack resistance during dissimilar welding. Comparing these electrodes provides useful information for selecting suitable filler metal for industrial applications.

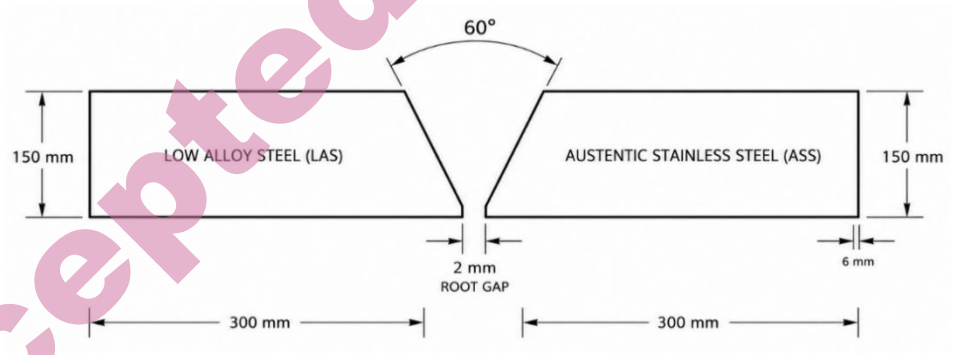


Figure 1. Schematic of plates weld joint



Figure 2. Welding of plates

Statistical analysis

For the reliability and repeatability of the experimental results three independent specimens were prepared and tested for each welding condition, including the as-welded condition and each PWHT temperature 600 °C, 615 °C, and 630 °C. The reported tensile properties ultimate tensile strength, yield strength, and elongation and Rockwell hardness values

Accepted manuscript

represent the mean ± standard deviation (SD) of the three measurements. The standard deviation was calculated using equation given below.

$$SD=\frac{\sqrt{\sum_{i=1}^{n}(xi-x)}}{n-1} \quad (1)$$

where *xi* is an individual measurement, $\bar{x}$ is the mean value, and *n* is the number of specimens tested. The relatively small standard deviations obtained in this study indicate good repeatability of the welding process, specimen preparation, heat treatment, and mechanical testing.

TABLE II. Chemical composition of electrode used by weight percentage

Constituents	E6013 (MS)	E308 (SS)
C	0.10	0.08
Mn	0.30-0.60	0.5 – 2.5
Si	0.20-0.35	0.90
S	0.035	0.03
P	0.040	0.03
Cr	-	19.0 – 21.0
Ni	-	9.0 – 11.0
Fe	balance	balance

Testing methods

Microstructural investigation provides detailed information regarding grain morphology and internal structural features and the internal irregularity which lead to failure. It is reported that a researcher Pandey found out the optimum heat treatment process for dissimilar joint between P92 steel and SS304 L by utilizing microstructure analysis in different portions of the weld sample.[22] A research team investigated to observe the correlation between microstructural analysis and mechanical properties in different PWHT processes and found out the efficient process for heterogeneous P91 welded joint.[23] In further research, both SEM and optical microscope have been used and observed the martensite structure in HAZ and austenitic structure in the welded zone.[24] The tensile properties were consistent with the observed microstructure. in the microstructural findings. In this study microstructure of base metals and heat-affected zone of both metals low alloy steel and Austenitic stainless steel structure was analyzed by using SEM. The magnification for SEM was 550x and 100x for the microstructural analysis sample size was 25 mm × 25 mm.

To determine which type of electrode and post-weld heat treatment (PWHT) are more suitable,[25] different types of destructive tests including tensile and Rockwell hardness tests have been performed. A tensile test was performed to find out the ultimate tensile strength, yield strength and percent of elongation of the test sample piece. To perform the tensile test Universal Tensile Testing Machine was used. The tensile test piece has been prepared and the test was performed by following ASTM E-8M standard. A Rockwell hardness test was performed to find the wear resistance and ductility of the test specimen. Rockwell hardness test gives the idea of whether post-weld heat treatment (PWHT) can have effect on the ductile property of the dissimilar weld joint.

For proper and good welding, welding parameters must be chosen according to the need of filler material and dissimilar joining. In this work of dissimilar joining the parameters which

Accepted manuscript

were selected are shown in Table III and also heat input was calculated by following given formula

$$\text{Heat Input} = \frac{V \times I \times 60}{1000 \times S} \quad (2)$$

TABLE III. Welding process parameters

Electrode type	Diameter (mm)	Pass No.	Current (A)	Voltage	Welding speed mm/min	Heat input (kJ/mm)
E6013 (MS)	3.2	1	110	24	180	0.88
		2	110	24	180	0.88
E308 (SS)	3.2	1	110	24	180	0.88
		2	110	24	180	0.88

RESULTS AND DISCUSSION

Microstructural examination using E6013 electrode

The microstructures of the base metals and heat-affected zones (HAZ) of the two dissimilar metals, welded using an E6013 electrode, were examined by SEM, as shown in the Figure 3 a, b

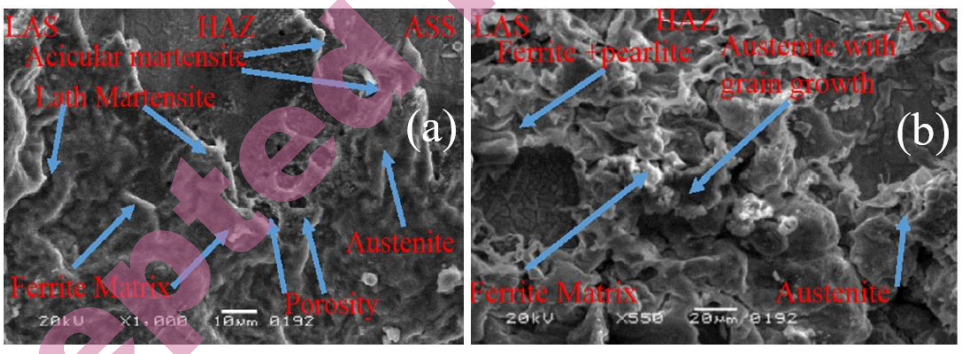


Figure 3 Microstructural Examination Using E6013 Electrode (a, b)

Figure 3(a) shows the SEM microstructure of the dissimilar welded joint between low alloy steel and austenitic stainless steel welded using E6013 welding electrode. The fusion zone revealed ferrite matrix formation along with acicular and lath martensitic structures. Minor porosity was also observed within the weld region. The heat-affected zones of both base metals exhibited microstructural transformation due to welding thermal cycles. Figure 3 (b) presents the SEM microstructure of the dissimilar weld joint showing ferrite and pearlite structures on the low alloy steel side, while the austenitic stainless steel side displayed an austenitic matrix with noticeable grain growth near the heat-affected zone. The identified microstructures show elemental diffusion and thermal influence during welding. The dissimilar welded joint showed irregular microstructures due to the difference in thermal conductivity and chemical composition of the base metals.

Accepted manuscript

The low alloy steel side primarily comprised of pearlite and ferrite phases, whereas the stainless steel side retained an austenitic structure. The development of martensite and ferrite in the weld metal is mainly determined by the relatively low nickel and chromium contents of the E6013 electrode, which offer minimal stabilization of the austenitic phase during cooling. Because AISI 4140 possesses comparatively high carbon content and hardenability, carbon diffusion from the low alloy steel into the fusion zone, together with the rapid cooling associated with SMAW promotes the transformation of austenite into martensite. The presence of martensite increases hardness but also introduces localized brittleness due to its internal residual stresses and high dislocation density. Therefore, although the E6013 electrode develops suitable joint strength, the weld is more susceptible to stress concentration and reduced ductility compared with stainless-steel electrode

Microstructural examination using E308 electrode

Figure 4(a) shows the SEM microstructure of the dissimilar welded joint developed using the E308 welding electrode. The weld metal showed an austenitic matrix containing δ-ferrite within interdendritic regions. Interdendritic segregation was observable due to chemical variation during solidification. The low alloy steel side primarily contained of pearlite and ferrite phases Figure 4(b) shows the microstructure of the weld region showing austenitic dendritic growth with δ-ferrite distributed along dendrite boundaries. The pearlite and ferrite structure was found on the low alloy steel side, verifying the heterogeneous microstructure development during dissimilar welding. The use of the E308 welding electrode improved the formation of austenitic dendritic weld metal with retained δ-ferrite, which is characteristic of stainless steel solidification behavior. The presence of δ-ferrite along dendrite boundaries improves resistance against solidification cracking, while interdendritic segregation occurred because of non-uniform elemental distribution during cooling.

In contrast, the greater nickel and chromium contents of the E308 electrode strengthen the austenitic phase during weld solidification and suppress excessive martensitic transformation. The retained δ-ferrite forms because the weld metal initially solidifies in the ferritic mode before partially transforming into austenite during cooling. A controlled amount of δ-ferrite is beneficial because it accommodates thermal stresses, reduces hot-cracking susceptibility, and improves weld integrity. Furthermore, the austenitic matrix provides greater plastic deformation capacity, explaining the superior ductility and tensile performance observed for the E308 welds.

Accepted manuscript

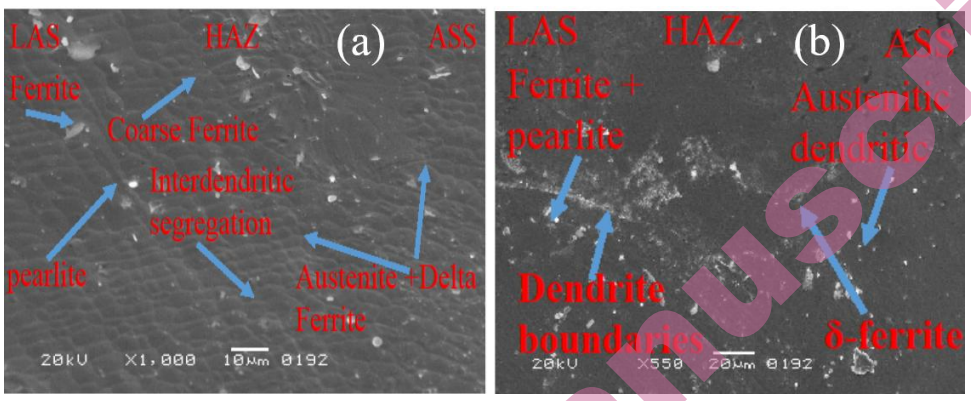


Figure 4. Microstructural examination using E308 electrode (a, b)

Mechanical properties

Tensile properties variation with E6013 Electrode.

The tensile properties of the dissimilar weld joint produced using the E6013 electrode showed a significant variation with post-weld heat treatment temperature. As welded samples exhibited an ultimate tensile strength (UTS) of 475 MPa, yield strength of 356 MPa, and elongation of 23%, indicating relatively lower ductility. After PWHT at 600 °C, slight improvements were observed where the UTS increased to 481 MPa and elongation increased to 27%. Further increase in PWHT temperature to 615 °C resulted in the highest tensile performance with UTS reaching 493 MPa, yield strength increasing to 370 MPa, and elongation improving to 34%, suggesting effective residual stress relief and tempering effects. However, when PWHT temperature increased to 630 °C, a slight reduction in mechanical properties occurred where UTS decreased to 486 MPa and elongation reduced to 30%, given in Table IV indicating possible softening effects at higher temperatures. The stress-strain curves shown in Figure 5 show that the sample treated at 615 °C indicated higher strain capacity and improved strength compared to the as welded condition, verifying the valuable effect of optimized PWHT on mechanical performance. After PWHT is primarily mainly attributed to residual stress relief and tempering of martensitic regions formed during welding increased in tensile properties. Tempering reduced internal stresses and transformed brittle microstructures into more stable tempered structures, thereby enhancing ductility while maintaining adequate strength. Furthermore, PWHT promoted a more uniform hardness distribution across the weldment, reducing stress concentration and improving load transfer during tensile loading.

Each tensile result presented in Table IV represents the average of three independent tests, and the error values correspond to one standard deviation, demonstrating good repeatability of the experimental procedure

Accepted manuscript

TABLE IV E6013 electrode tensile results

Condition	UTS (MPa)	Yield strength (MPa)	Elongation (%)
As Welded	475± 2.65	356± 2.31	23%
PWHT 600 °C	481± 2.00	361± 2.00	27%
PWHT 615 °C	493± 1.15	370± 2.00	34%
PWHT 630 °C	486± 2.65	365± 2.65	30%

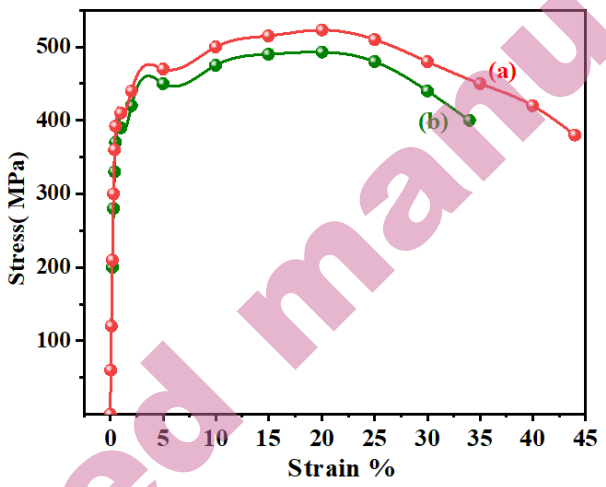


Figure 5. Stress strain curve of LAS-ASS dissimilar joint on (a) as welded condition with E6013 Electrode (b) PWHT at 615 ºC with E6013 electrode

Tensile properties variation with E308 electrode

The dissimilar welded joint fabricated using the E308 electrode exhibited superior tensile properties compared to the E6013 electrode under all conditions. The as-welded sample produced a UTS of 498 MPa, yield strength of 374 MPa, and elongation of 33%. Given in Table V. Application of PWHT at 600 °C improved the tensile behavior where UTS increased to 508 MPa and elongation reached 37%. The optimum mechanical performance was achieved at PWHT 615 °C, where the joint attained the highest UTS of 523 MPa, yield strength of 392 MPa, and elongation of 44%. The improved mechanical properties can be associated with stress relief and stabilization of the weld microstructure. Increasing the PWHT temperature to 630 °C resulted in a minor decrease in tensile strength to 514 MPa, although ductility remained relatively high at 42%. Figure 6 stress-strain curves reveal that the specimen treated at 615 °C exhibited greater plastic deformation and higher load-bearing capability compared to the as-welded condition, confirming that E308 combined with optimized PWHT produced the most favorable mechanical behavior for the dissimilar weld joint

Accepted manuscript

TABLE V E308 electrode tensile results

Condition	UTS (MPa)	Yield strength (MPa)	Elongation (%)
As Welded	498± 2.00	374± 0.00	33%
PWHT 600 °C	508± 2.00	381± 2.00	37%
PWHT 615 °C	523± 3.06	392± 3.00	44%
PWHT 630 °C	514± 2.08	386± 2.65	42%

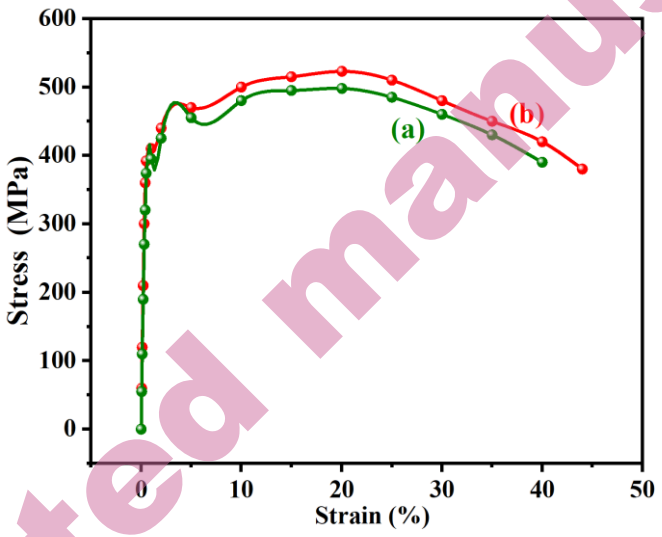


Figure 6. Stress strain curve of LAS-ASS Dissimilar joint on (a) as welded condition with E308 Electrode (b) PWHT at 615 ºC with E308 electrode

Among all PWHT conditions, 615 °C formed the optimum mechanical performance because it effectively relieved residual stresses generated during welding without causing excessive grain coarsening. At 600 °C the tempering effect remained no effect on the properties of dissimilar weld joint, whereas increase to 630 °C initiated slight over-tempering, leading to minor reductions in tensile strength. The better tensile performance of the E308 welds results from the combined effects of an austenitic weld matrix and optimized post-weld heat treatment. The nickel and chromium rich weld metal possesses greater toughness and accommodates plastic deformation more effectively than the ferritic martensitic weld produced by E6013. PWHT at 615 °C provided sufficient thermal energy to relieve welding residual stresses and stabilize the weld microstructure without causing excessive softening. Consequently, crack initiation was delayed, strain distribution became more uniform, and the joint exhibited the highest tensile strength and elongation. When the PWHT temperature increased to 630 °C, over-tempering reduced dislocation density and promoted slight grain coarsening,

Accepted manuscript

explaining the small decrease in strength despite the retention of relatively high ductility.

Hardness of E6013 welded dissimilar joint

Hardness testing was conducted using the Rockwell C (HRC) scale in compliance with ASTM E18. A 120° diamond cone indenter and a total test load of 150 kgf (10 minor load and 140 major load) were used. Hardness measurements were obtained after maintaining the applied load for the standard dwell period specified by the testing procedure. Three readings were taken at each measurement location, and the average value was reported according to each location shown in Figure 7

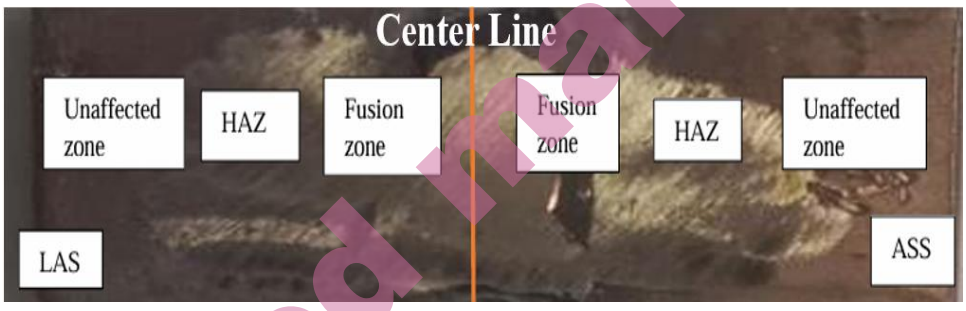


Figure 7, Hardness test welded sample

Hardness measurements at each location were repeated three times, and the reported values correspond to the arithmetic mean ± standard deviation. The low variation among repeated measurements confirms the consistency of the hardness distribution throughout the welded joints. The hardness distribution across the dissimilar AISI 4140 and AISI 201 welded joint fabricated using the E6013 electrode is presented in Figure 8. In the as welded condition, the highest hardness was observed in the LAS heat-affected zone 46.2 ± 0.66 HRC, followed by the weld fusion zone on the LAS side 38.5 ± 0.82 HRC, indicating the formation of a harder microstructure due to rapid cooling during welding. The weld center exhibited an intermediate hardness of 32.3 ± 0.66 HRC, while the ASS HAZ and unaffected zones showed comparatively lower hardness values.

Post-weld heat treatment resulted in a significant reduction in hardness throughout the weldment. At 600 °C, the LAS HAZ hardness reduced to 39.1 ± 0.75 HRC, while furthermore reductions were noted at 615 °C 31.2 ± 0.80 HRC. The minimum hardness values were mainly observed at 615 °C, indicating effective tempering and stress relief of the weld region. At 630 °C, a minor increase in hardness was recorded in many regions, particularly in the LAS HAZ 35.4 ± 0.80 HRC and weld center 27.1 ± 0.56 HRC, which may be related to microstructural control during heat treatment.

Accepted manuscript

Overall, PWHT efficiently reduced hardness gradients throughout the weldment, resulting in a more similar hardness profile. The reduction in hardness is indicative of decreased residual stresses and improved metallurgical stability within the welded joint. The high hardness observed in the as welded condition is mainly associated with martensite formation in the heat-affected zone of AISI 4140. Owing to the high carbon content of the steel and rapid cooling during welding, carbon becomes trapped within the martensitic structure, producing high hardness but reduced toughness. PWHT progressively tempers this martensite, allowing carbide precipitation and reducing residual stresses. Consequently, hardness decreases significantly as the PWHT temperature increases to 615 °C. The slight increase in hardness at 630 °C may be associated with microstructural stabilization and secondary carbide precipitation during prolonged tempering.

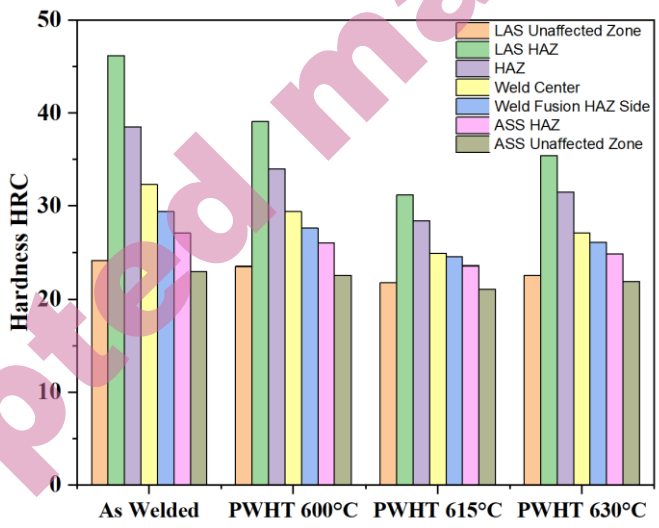


Figure 8. Comparative hardness result E6013 electrode

Hardness of E308 welded dissimilar joint

The hardness values for the dissimilar AISI 4140 and AISI 201 welded joint produced using the E308 electrode are summarized in Figure 9. Similar to the E6013 weldment, the highest hardness in the as-welded condition was recorded in the LAS heat-affected zone 42.5 ± 0.80 HRC, followed by the weld fusion zone on the LAS side 34.1 ± 0.80 HRC. The weld center and ASS side regions exhibited lower hardness values, reflecting the influence of the austenitic stainless steel electrode and associated microstructural characteristics. Following post-weld heat treatment, hardness values decreased progressively in all regions. The LAS HAZ hardness decreased from 42.5 ± 0.80 HRC in the as-welded condition to 36.3 ± 0.80 HRC at 600 °C and further to 29.4 ± 0.80 HRC at 615 °C. The weld center

Accepted manuscript

hardness also declined from 26.0 ± 0.80 HRC to 21.2 ± 0.85 HRC at 615 °C. A minor improvement in hardness was noted after PWHT at 630 °C, where the LAS HAZ reached 33.0 ± 0.66 HRC and the weld center increased to 22.8 ± 0.80 HRC.

The results demonstrate that PWHT effectively softened the weld and heat-affected regions by promoting stress relief and microstructural tempering. Compared with the E6013 electrode, the E308 weldment exhibited generally lower hardness values throughout the weld zone, which can be attributed to the austenitic nature of the electrode. This behavior is beneficial for reducing brittleness and improving the toughness of the dissimilar welded joint.

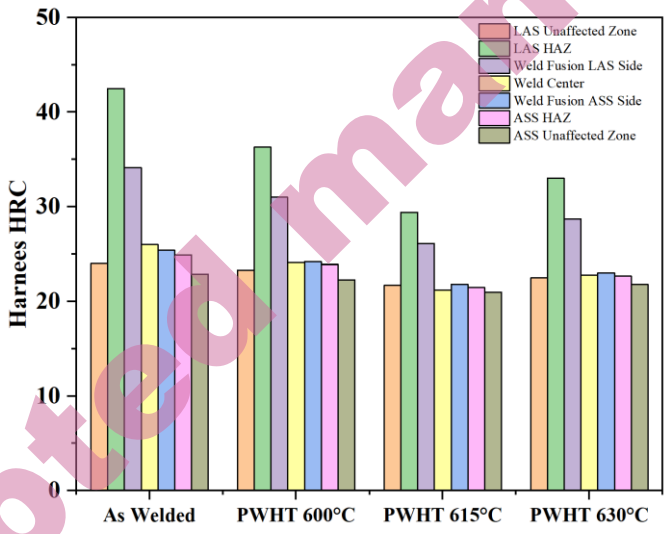


Figure 9. Comparative hardness result E308 Electrode

CONCLUSION

The present study investigated the effect of electrode selection and PWHT on the microstructure and mechanical properties of SMAW-based dissimilar weld joints between AISI 4140 low alloy steel and AISI 201 stainless steel. On the basis of experimental findins, the following conclusions can be drawn:

1. Electrode selection significantly influenced the weld microstructure and mechanical properties. SEM observations revealed ferritic and martensitic features in the E6013 weld metal, whereas E308 produced an austenitic dendritic microstructure containing retained δ-ferrite
2. PWHT improved the tensile properties of the welded joints, with 615 °C providing the best overall mechanical performance among the investigated heat-treatment temperatures.

Accepted manuscript

3. The E308 electrode combined with PWHT at 615 °C achieved the highest tensile properties, with an ultimate tensile strength of 523 MPa, yield strength of 392 MPa, and elongation of 44%
4. Hardness measurements showed variations across the welded joint after PWHT, particularly in the low-alloy steel heat-affected zone and weld metal. These changes demonstrate the influence of PWHT temperature on the hardness distribution
5. Overall, E308 combined with PWHT at 615 °C provided the most favorable balance of tensile properties and hardness characteristics for SMAW dissimilar welding of AISI 201 stainless steel and AISI 4140 low-alloy steel.

Limitations and future work

Although the present study provides valuable insights into the combined effects of E6013 and E308 electrode and post-weld heat treatment on the microstructure and mechanical properties of SMAW dissimilar AISI 201 and AISI 4140 welded joints, several limitations should be acknowledged. The investigation was limited to the SMAW process, two commercially available electrodes E6013 and E308, and three PWHT temperatures 600 °C, 615 °C, and 630 °C with a constant holding time of 1 h. Furthermore, the study focused on microstructural characterization, tensile properties, and hardness, while long-term performance aspects such as corrosion resistance, fatigue behavior, fracture toughness, wear resistance, and detailed fracture surface analysis were beyond its scope. Future research should evaluate additional welding processes, alternative electrodes, a wider range of PWHT conditions, and comprehensive service performance characteristics to further optimize dissimilar weld joints for industrial applications.

И З В О Д

УТИЦАЈИ ТЕРМИЧКЕ ОБРАДЕ НАКОН ЗАВАРИВАЊА НА СПОЈЕВЕ РАЗЛИЧИТИХ ЧЕЛИКА AISI 201/4140

SHOUKAT ALI NOONARI[1*], ABDUL SATTAR JAMALI[1], QADIR BAKHSH JAMALI[1], ABDUL QADEER LAGHARI[2†], IMDAD ALI[1], HAMZA SHAIKH[3], SAGHEER AHMED[4], MUHAMMAD SHUAIB SHAIKH[2], ARSHAD IQBAL[5], и MASROOR ABRO[2]

[1]Mechanical Engineering Department, Quaid-e-Awam University of Engineering and Technology, Nawabshah, Pakistan, [2]Chemical Engineering Department, Mehran University of Engineering and Technology, Jamshoro, Sindh, Pakistan, [3]Mechanical Engineering Department, Mehran University of Engineering and Technology, Jamshoro, Sindh, Pakistan, [4]Mechanical Engineering Department, Isra University Hyderabad, Sindh, Pakistan, и [5]Chemical Engineering Department, Dawood University of Engineering and Technology, Karachi, Sindh, Pakistan.

Заваривање аустенитног нерђајућег челика и нисколегираног челика широко се примењује код посуда под притиском, у петрохемијским постројењима, системима за производњу енергије и конструкцијама, јер обједињује отпорност на корозију нерђајућег челика и велику чврстоћу нисколегираног челика. Међутим, добијање висококвалитетних заварених спојева представља изазов због разлика у топлотном ширењу, хемијском саставу и микроструктурним променама. У овом раду испитује се заједнички утицај избора

Accepted manuscript

електроде и термичке обраде након заваривања (PWHT) на микроструктуру и механичка својства спојева нисколегираног челика AISI 4140 и аустенитног нерђајућег челика AISI 201 изведених ручним електролучним заваривањем (SMAW). Узорци су заварени употребом електрода E6013 и E308, а затим су подвргнути термичкој обради PWHT на температурама од 600 °C, 615 °C и 630 °C у трајању од 1 сата, након чега је уследило хлађење у пећи. Микроструктурна анализа спроведена је помоћу скенирајуће електронске микроскопије (SEM), док су за процену механичких карактеристика заварених спојева извршена испитивања затезањем и мерење тврдоће по Роквелу. SEM карактеризација је показала да се у зони топљења спојева изведених електродом E6013 формирају феритно-мартензитне структуре, док се при употреби електроде E308 формира аустенитна дендритна микроструктура која садржи заостали δ-ферит. Уочено је да је након термичке обраде PWHT дошло до смањења варијација у тврдоћи и побољшања својстава при затезању. Међу испитиваним узорцима, најбоље механичке карактеристике показао је узорак заварен електродом E308 и термички обрађен на 615 °C, постигнута је затезна чврстоћа од 523 MPa, напон течења од 392 MPa и издужење од 44%. Ова побољшања су резултат ефикасног смањења заосталих напона и стабилизације микроструктуре током термичке обраде. Резултати показују да комбинација употребе електроде E308 и термичке обраде на 615 °C пружа најповољнији баланс механичких својстава и микроструктурне стабилности при ручном електролучном заваривању SMAW различитих челика, AISI 4140 и AISI 201.

(Примљено 28. августа; ревидирано 10. септембра; прихваћено 28. октобра 2026.)

REFERENCES

1. Y. Wang, K. Sebeck, E. Gingrich, M. Tess, J. A. Haynes, G. Muralidharan, K. Will, D. Pierce, *J. Mater. Res. Technol.* **39** (2025) 8340 (https://doi.org/10.1016/j.jmrt.2025.11.108)
2. A. Garga, A. Verma, S. Kumar, V. Badheka, Hirshikesh, C. Pandey, *Mater. Today Commun.* **52** (2026) 115006 (https://doi.org/10.1016/j.mtcomm.2026.115006)
3. R. M. Afify, T. S. Mahmoud, A. O. Mosleh, M. Abdelal, *Int. J. Precis. Eng. Manuf.* **27** (2026) 1005 (https://doi.org/10.1007/s12541-025-01374-8)
4. R. A. Fouad, M. I. A. Habba, Y. G. Y. Elshaghoul, M. M. El-Sayed Seleman, K. M. Hafez, H. Hemdan El-Fahhar, W. S. Barakat, *Sci. Technol. Weld. Join.* **29** (2024) 356 (https://doi.org/10.1177/13621718241283374)
5. N. Çavuşoğlu, *J. Mater. Eng. Perform.* **31** (2022) 4035 (https://doi.org/10.1007/s11665-021-06474-w)
6. V. T. Gaikwad, I. Balasundar, A. Tripathi, R. K. P. Singh, M. K. Mishra, *Mater. Sci. Technol.* **40** (2024) 909 (https://doi.org/10.1177/02670836241231480)
7. S. Manzoor, M. Tahir, R. A. Karim, J. Xiong, M. I. Khan, *Surf. Rev. Lett.* **30** (2023) 2350042 (https://doi.org/10.1142/S0218625X23500427)
8. M. Abbas, G. A. Bastawesy, H. A. Abdel-Aleem, *Egypt. J. Chem.* **68** (2025) 75 (https://doi.org/10.21608/ejchem.2025.341621.10931)
9. A. K. Maurya, R. Chhibber, C. Pandey, *J. Mater. Sci.* **58** (2023) 8597 (https://doi.org/10.1007/s10853-023-08562-9)
10. N. Arivazhagan, S. Singh, S. Prakash, G. M. Reddy, *Mater. Des.* **32** (2011) 3036 (https://doi.org/10.1016/j.matdes.2011.01.037)
11. S. B. Jamaludin, M. N. Mazlee, S. K. A. Kadir, K. R. Ahmad, *Adv. Mater. Res.* **795** (2013) 74 (https://doi.org/10.4028/www.scientific.net/AMR.795.74)

Accepted manuscript

12. S. Kumar, C. Pandey, A. Goyal, *Int. J. Press. Vessel. Pip.* **185** (2020) 104128 (https://doi.org/10.1016/j.ijpvp.2020.104128)
13. C. Pandey, *Metall. Mater. Trans. A* **51** (2020) 2126 (https://doi.org/10.1007/s11661-020-05660-0)
14. R. Mittal, B. S. Sidhu, *J. Mater. Process. Technol.* **220** (2015) 76 (https://doi.org/10.1016/j.jmatprotec.2015.01.008)
15. L. Y. Narayan, V. Bhanu, S. Sirohi, S. Kumar, D. Fydrych, C. Pandey, *Int. J. Adv. Manuf. Technol.* **140** (2025) 2129 (https://doi.org/10.1007/s00170-025-16361-6)
16. A. K. Maurya, A. Bhattacharyya, R. Chhibber, C. Pandey, *Mater. Chem. Phys.* **318** (2024) 129322 (https://doi.org/10.1016/j.matchemphys.2024.129322)
17. A. Garga, S. Sirohi, D. Fydrych, C. Pandey, *Int. J. Adv. Manuf. Technol.* **144** (2026) 5493 (https://doi.org/10.1007/s00170-026-18179-2)
18. M. Maheshwari, A. Garga, K. Gupta, S. Kumar, P. Kumar, C. Pandey, *Arch. Civ. Mech. Eng.* **26** (2026) 136 (https://doi.org/10.1007/s43452-026-01506-5)
19. T. Zhang, W. Wang, J. Zhou, Z. Yan, J. Zhang, *J. Manuf. Process.* **42** (2019) 257 (https://doi.org/10.1016/j.jmapro.2019.04.031)
20. P. Kah, M. Shrestha, J. Martikainen, *Appl. Mech. Mater.* **440** (2014) 269 (https://doi.org/10.4028/www.scientific.net/AMM.440.269)
21. D. Liu, J. Wang, M. Xu, H. Jiao, Y. Tang, D. Li, L. Zhao, S. Han, *J. Manuf. Process.* **58** (2020) 500 (https://doi.org/10.1016/j.jmapro.2020.08.031)
22. B. Chen, H. Xiong, B. Sun, S. Tang, B. Du, N. Li, *Prog. Nat. Sci. Mater. Int.* **24** (2014) 313 (https://doi.org/10.1016/j.pnsc.2014.06.003)
23. M. P. Nascimento, R. C. Souza, W. L. Pigatin, H. J. C. Voorwald, *Int. J. Fatigue* **23** (2001) 607 (https://doi.org/10.1016/S0142-1123(01)00015-9)
24. N. Arivazhagan, S. Singh, S. Prakash, G. M. Reddy, *Mater. Sci. Eng. B* **132** (2006) 222 (https://doi.org/10.1016/j.mseb.2006.02.047)
25. G. F. Li, E. A. Charles, J. Congleton, *Corros. Sci.* **43** (2001) 1963 (https://doi.org/10.1016/S0010-938X(00)00182-7)

Accepted Manuscript